Geotomography Trials on the Edge of the Australian and European Plates

Agus Abdullah[1], Cvetan Sinadinovski[2], Lazo Pekevski[3] and Kevin F. M[c]Cue[4]

1. Corresponding Author. Geophysical Engineering, Pertamina University, Indonesia. Email: agusabdullah@gmail.com
2. Global Seismics, ACT, Australia. Email: cvetansin@hotmail.com
3. Seismological Observatory, University "Ss. Cyril and Methodius" (UKIM), Skopje, Macedonia. Email: lazopekevski@yahoo.com
4. Central Queensland University, Rockhampton, Qld., Australia. Email: mccue.kevin@gmail.com

Abstract

A novel geotomography technique has been applied using data from two different regions of the world. The aim was to test this new method for investigation of the crustal shape and structure in specific tectonic regions where significant datasets have been acquired.

In the first study, near-field P and S travel times were tomographically inverted from more than a hundred aftershocks recorded in Papua New Guinea on 6 accelerographs deployed in the epicentral zone of the magnitude M7.5 earthquake on February 26th 2018. In the second study, selected earthquakes that occurred over a period of 40 years and were recorded on 47 stations across Macedonia, were used in a geotomography experiment.

Three dimensional models and many cross-sections of the crust were produced by this new methodology in both cases. They show the potential of the geotomography application in revealing velocity perturbation on local and regional scales. The new images will contribute towards a better understanding of the seismotectonics in the regions and improvement of earthquake hazard assessments.

Keywords: earthquakes, aftershocks, travel times, geotomography

1 INTRODUCTION

The intention of these trials was to test the potential of the new geotomographic method for investigation of the crustal shape and structure in specific tectonic regions with extensive datasets. By definition, geotomography is the adaptation of computer aided tomography (CAT) scan technology to the analysis of geologic features such as rock types. The geotomography technique analyses the ray paths between a source and receiver which are positioned at various locations on Earth. Various types of waves, such as seismic, acoustic, electromagnetic, or X-rays, can be analysed by the computer software to create images of the medium. For the purpose of this study, passive seismic experiments were considered with naturally occurring earthquakes as sources and the phase arrival information acquired at seismograph stations. In seismic tomography, the time of the seismic waves travelling between the origin of the earthquake and the station is measured and used in the inversion process, referred to as travel-time inversion.

2 METHOD

The technique presented here is designed for travel-time tomography. The surveyed volume, a cuboid, was discretised into cells of chosen grid size on the surface and depth ranges over set intervals. Within the cuboid, for each source-receiver i.e. earthquake-station combination the traveltime was calculated based on the initial velocity model. Such calculated arrivals were compared with the observed arrivals on the seismograms, commonly for the P and S phases.

The tomography images are stored as a matrix of slowness perturbations in respect to the initial 3D velocity model (Kennett and Abdullah, 2011). The velocity matrix values can also be graphically shown at various slices through the cuboid , typically horizontally and vertically. The novelty of this technique is its ability to be applied simultaneously in forward modelling and upgrading, thus allowing the user to monitor in 3-D space the effects of the re-location of seismic events on the model composition.

This tomographic inversion is performed using irregular grid parametrization (Fig. 1a). A tetrahedron cell discretization of complex geological models is especially useful in situations of rough topography and high-contrast anomalies. The program works with numerous source and receiver combinations. The standard checker-board tests show that the recovered images are stable and improved in comparison with the regular models.

Tetrahedron ribs are utilized for ray tracing that are five times finer at shallow depths and coarser at greater depth (Fig. 1b). Source and receiver locations are embedded into the ribs to enable ray tracing between each source and receiver pair. This technique preserves geometry with narrow offset (local earthquakes) while maintaining distant earthquakes and reasonable computation time. Furthermore, the tree for finding the K-nearest neighbours of a specific number of locations is used as a technique to optimize the Dijkstra algorithm during searching for the fastest path that fulfils the Fermat principle.

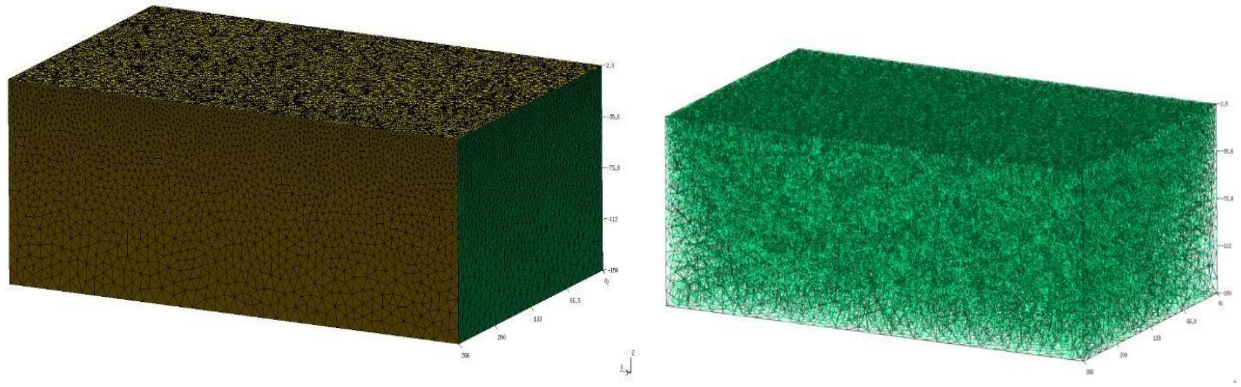

a) b)

Figure1: Schematic representation of a) parametrization and b) tetrahedron ribs used for ray tracing. (Model size is relative and numbers can be scaled up or down)

Therefore, forward models are more realistic and the resulting images of the sub-structures can indicate variations in the velocity with a higher degree of confidence. The new geotomography images will show the potential of the methodology in revealing more detailed velocity perturbation at local and regional scales. This experimental work is on-going and the computer code is being tested in different tectonic environments.

3 EXAMPLES

In the first part of this study, the geotomographic technique was applied to a dataset comprising seismic records from the Papua New Guinea Southern Highland region, acquired after the magnitude M7.5 earthquake of February 26th 2018. In the second case, selected earthquakes that occurred over a period of 40 years and were recorded on 47 stations across Macedonia in South Eastern Europe, were used in a geotomography experiment. The new images from both trials are compared with the results produced by other methods and analysed in respect to the seismicity and tectonic maps in the regions.

3.1 SEISMIC TOMOGRAPHY UNDER THE SOUTHERN HIGHLANDS OF PNG

The geotomography software was used to calculate the near-field P and S travel times from more than a hundred aftershocks recorded in Papua New Guinea on 6 accelerographs and to constrain velocity/depth relationships in the fault zone of the February 26th 2018 major earthquake. The datasets consisted of 3-component strong motion records recovered from the network for a M6.3 aftershock and hundreds of smaller events. Data from the largest aftershock recorded on 7th of April 2018 was available through the Australian Earthquake Engineering Society website www.aees.org.au website (Sinadinovski *et al.*, 2019).

To explore the crust under the Southern Highlands of PNG, aftershocks that occurred in a cuboid of 2x2 degrees centered on the temporary network and down to 60km deep were processed. To investigate the 3-D structure underneath the area, an initial velocity model (Gibson *et al.*, 2018) was utilised as shown in Table 1. The main goal was to evaluate the top layers and estimate the depth to the Moho discontinuity.

Table 1: Modified Gippsland model, P and S velocities versus depth, used for aftershock locations.

Depth (km)	Vp (km/s)	Vs (km/s)
0-3	3.802	2.398
3-8	5.521	3.413
8-20	6.052	3.572
20-45	6.240	3.661
45-60	7.812	4.460

The volume was discretised into cells of 15kmx15km over the surface area and depth ranges in the intervals of 3, 8, 15, 20, 28, 35, and 45 to 60km. After reviewing the seismograms, over 100 events were selected based on their origin in depth and azimuth in respect to the location of the network. Hence, between 500 and 600 P-arrival times and corresponding S-arrival times were used in the tomographic analysis. The ray paths and the coverage for the events and the recording stations over the topography of the study area are schematically presented in Figure 2. The cuboid has relatively good angular coverage in the area of interest and down to 45km, as there are only a few deeper events.

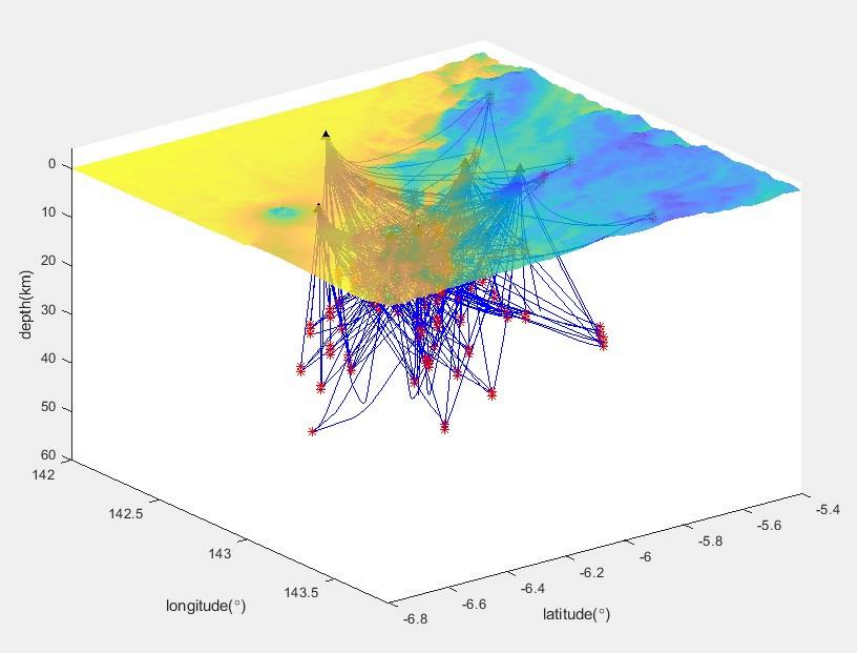

Figure 2: The ray paths and the coverage for the events and the receivers with the topography of the study area (earthquakes-red stars, stations-black triangles, ray paths-blue lines).

3.2 SEISMIC TOMOGRAPHY OF MACEDONIA

The geotomography software was used to invert regional P and S travel times from around 780 chosen earthquakes recorded on 47 selected seismic stations in Macedonia, in South Eastern Europe. The location of the seismic stations and the political borders are shown on Fig. 3.

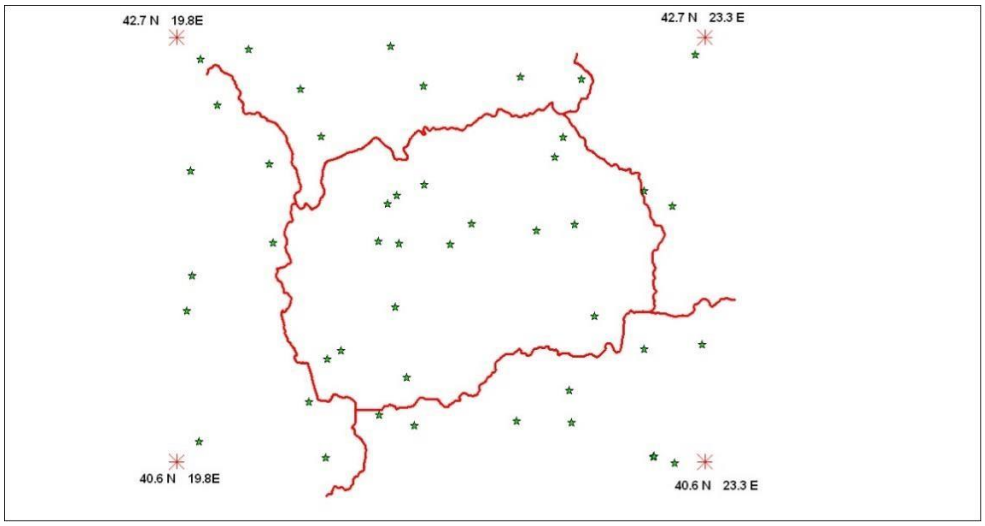

Figure 3: The location of the 47 selected seismic stations used in the experiment in and around Macedonia.

The input datasets consisted of earthquakes that occurred over the last 40 years across Macedonia (Fig. 4). They were chosen for the strongest events in each particular depth range and the biggest number of corresponding seismogram readings.

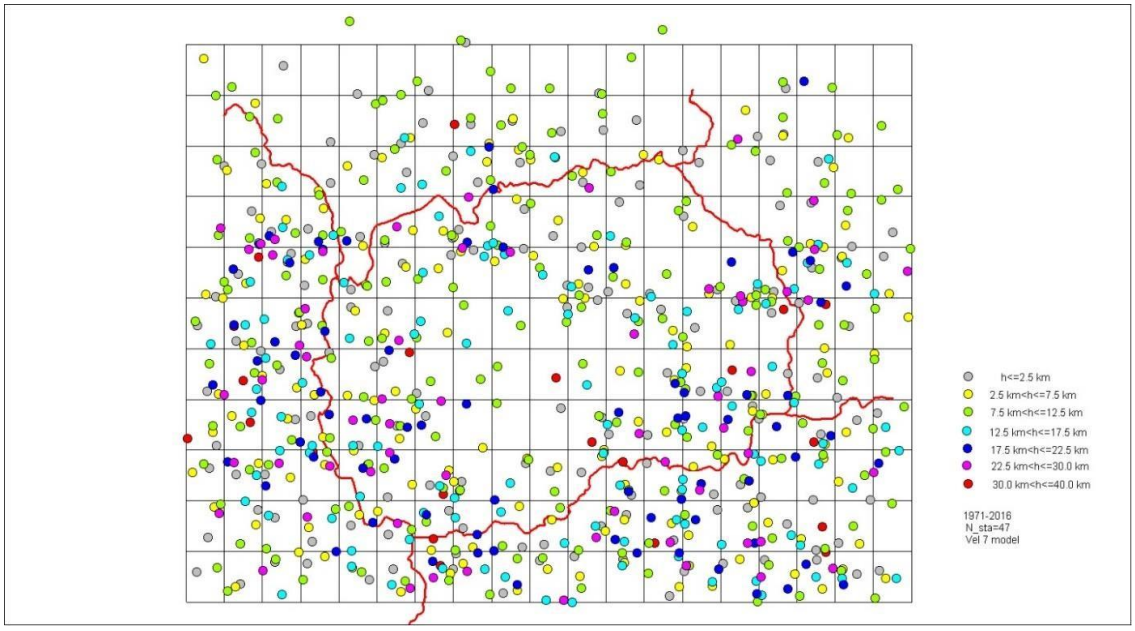

Figure 4: The location of the chosen seismic events (circle colours represent depth).

To explore the regional lithosphere under Macedonia, the events that occurred in a cuboid of 19.5E to 23.5E degrees and 40.5N and 43N degrees and down to 60km deep were processed. To investigate the 3-D structure underneath the area, the initial velocity model (after Pekevski *et al.*, 2009) was utilised as shown in Table 2. Again, the aim was to use the data to better image the top layers and evaluate the depth of the Moho discontinuity.

Table 2: Velocity model used for Macedonia.

Depth (km)	Vp (km/s)	Vs (km/s)
0-5	4.4	2.54
5-10	5.1	2.95
10-15	6.2	3.58
15-20	6.5	3.757
20-30	6.9	3.988
30-45	7.7	4.45

The volume was discretised into cells over a 17.5kmx17.5km grid in surface area and depth intervals at 5, 10, 15, 20, 30, and 45 to 60km. By reviewing the seismological reports from the catalogue, over 780 earthquakes were selected due to their focal distribution in depth and azimuth in respect to the location of the 47 stations. More than 7000 P-arrivals and equivalent number of S-arrival times were used in the tomographic analysis. The ray paths and the coverage for the events and the recording stations over the topography of the study area are schematically presented in Figure 5. The cuboid has relatively homogeneous angular coverage across the area and down to 45km, where the majority of the earthquakes occurred.

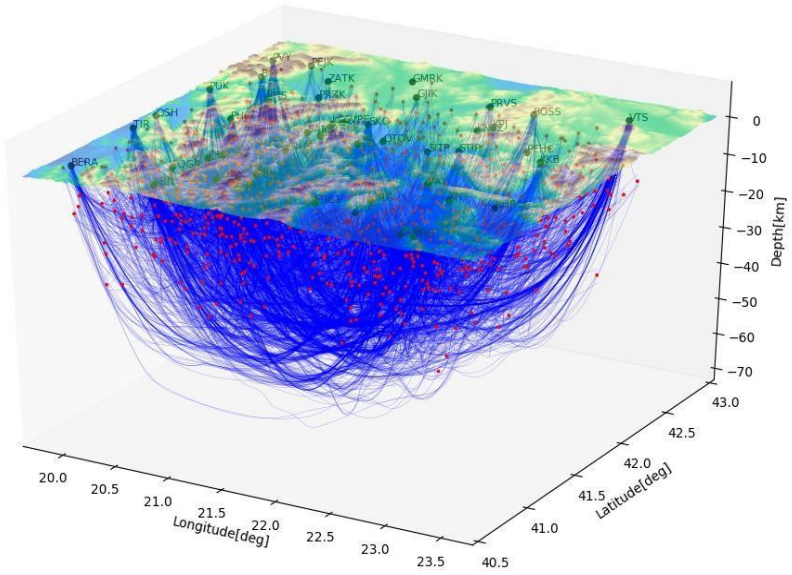

Figure 5: The ray paths and the coverage for the events and the stations over the topography of Macedonia (earthquakes-red stars, stations-black triangles, ray paths-blue lines).

4 TOMOGRAPHY RESULTS

First, the near-field P and S travel times were tomographically inverted for the area in Papua New Guinea as described in section 3.1. These were followed by the geotomography images for the region of Macedonia in South Eastern Europe, with parameters defined in section 3.2. Three dimensional corrections to the crustal model were obtained and displayed as slowness perturbations in respect to the initial velocity.

4.1 SEISMIC IMAGING UNDER THE SOUTHERN HIGHLANDS OF PNG

The tomography results are displayed as P- and S-wave slowness perturbations in respect to the initial velocity model given in Table 1 at various slices through the cuboid. The rainbow colour bar represents blue-fast and yellow-slow values, while the recovered images can be viewed with confidence only in the cells crossed by the seismic rays, as indicated by the preceding checkerboard tests.

The number of iterations versus relative residual and the corresponding P-wave and S-wave tomographic images was monitored and displayed in parallel. The iteration stops when it is convergent and stable, usually around values equivalent to the reading error of the phase arrivals. Figure 6 shows the relative S-wave slowness perturbation in respect to the initial checkerboard model at depths between 20 and 27 km. In that situation, assuming that the precision of reading the arrivals is 0.1 s, the inversion process can be stopped after 4 iterations.

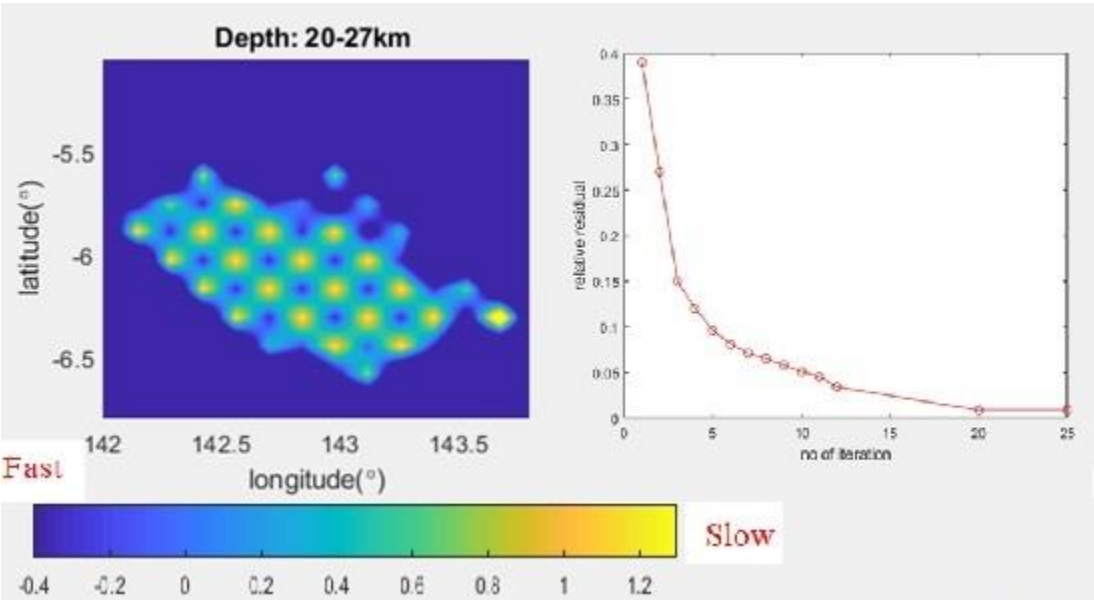

Figure 6: Recovered checkerboard image and the number of iterations versus slowness residual at a depth range of 20-27km.

Various depths and wave combinations are possible, here a subset was chosen that represents the area of our research interest. Figure 7 shows the relative S-wave slowness perturbation in respect to the initial velocity model at depths between 0 and 60 km.

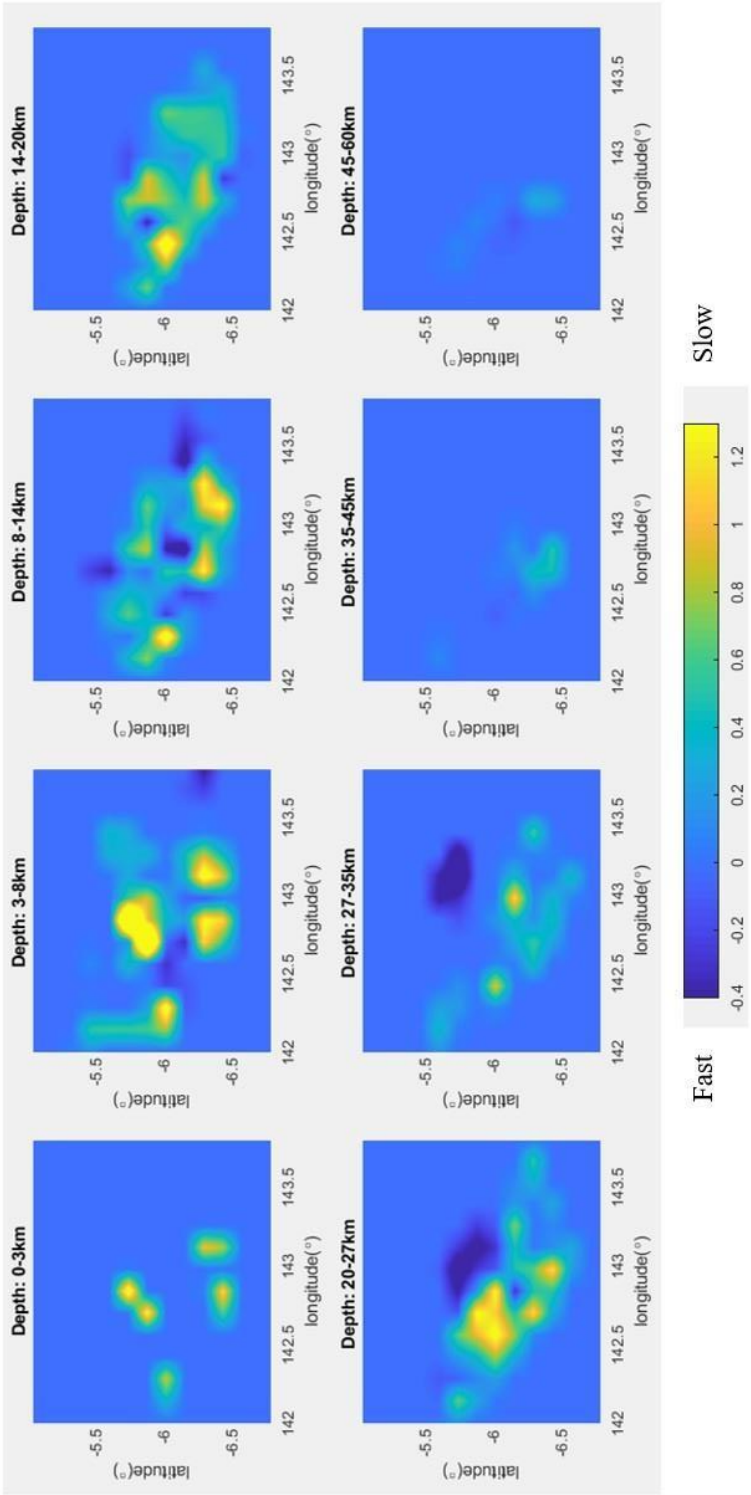

Figure 7: Horizontal S-wave slowness perturbation images at various depths.

Figure 8 shows tomographic images on longitudinal and latitudinal vertical slices and middle horizontal slice through the cuboid, as slowness perturbation. Slices can be chosen to be either orthogonal or at any desired angle.

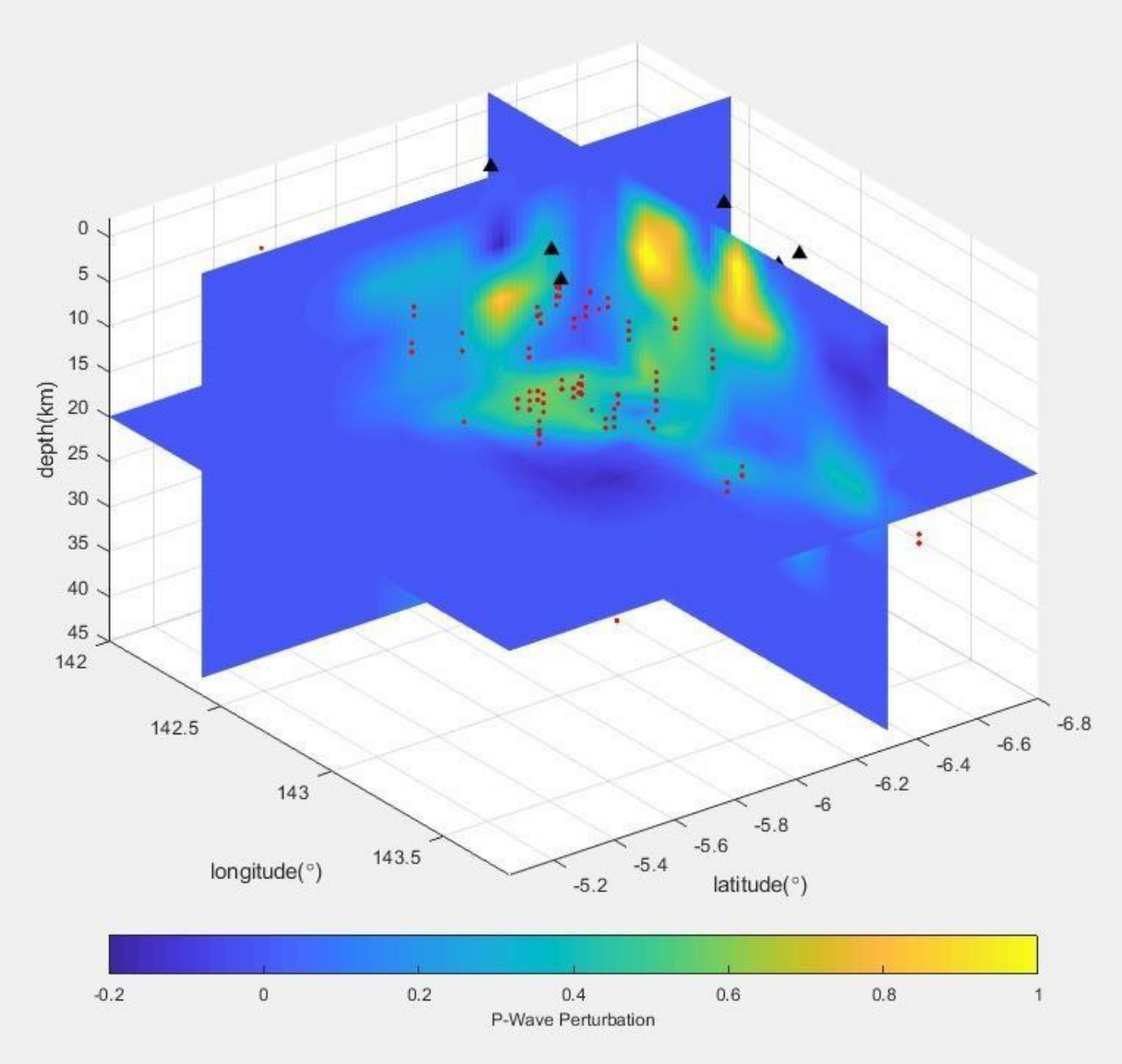

Figure 8: Combined images of two orthogonal vertical slices (N-S and E-W) and the middle horizontal slice through the cuboid as P-wave slowness perturbation; events are denoted by red stars and stations by black triangles.

Horizontal images produced using the P- and S-arrivals look very similar, due to the fact that the number of readings used in the inversion was very close in both cases. The zone of velocity anomalies in general have a NW-SE trend, which is consistent with the general direction of the PNG highlands. On both the north and south side of that zone, there are shallow discontinuous blocks with slower velocity of up to 1 km/s. Such velocity zones on the images might resemble the situation of compression from the north and south, with a gently folded belt in between.

The most northerly E-W slices and the most westerly N-S slices through the cuboid have little data to change the background velocity. The results for the vertical slices through the cuboid within the station network can be viewed with higher confidence. From the combined images a low velocity

zone coinciding with the known volcano Mt. Bosavi appeared on the southern side, with its imprint extending down to 20 km. Yet, since its external part is not well crisscrossed by the rays, some deeper sections may be subject to the artefacts of the tomography (Sinadinovski *et al.*, 2019).

4.2 SEISMIC IMAGING OF MACEDONIA

Again, the tomography results are displayed as P-wave and S-wave slowness perturbations in respect to the initial velocity model given in Table 2 at various slices through the cuboid. The rainbow colour bar represents blue-fast and red-slow values, while the recovered images can be viewed with confidence only in the cells crossed by the seismic rays multiple times.

The number of iterations versus relative residual and the corresponding tomographic images were monitored and displayed too. The inversion process can be set to stop when the differences between the observed and calculated time are convergent and stable, usually between 5 and 10 iterations.

Figure 9 shows the results of the checkerboard test as slowness perturbation in respect to the initial velocity model at a depth range of 10-15 km, when the inversion stopped after 5 iterations.

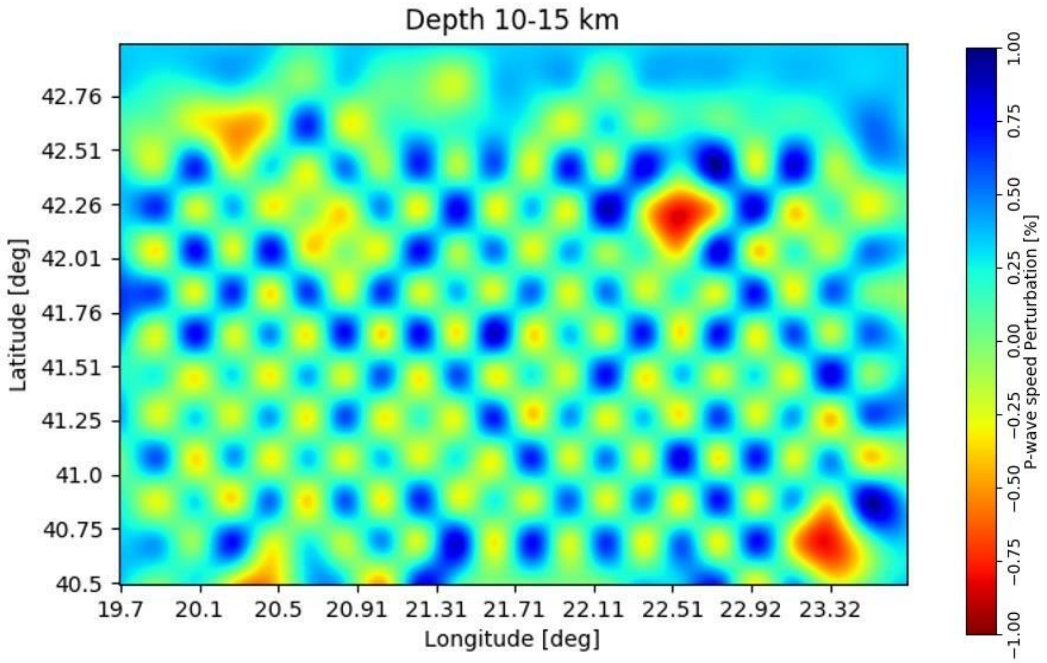

Figure 9: Example of the checkerboard tests for the layer between 10 and 15 km.

Various depths and cross-sections combinations were considered. On Figure 10 we show the horizontal P-wave and S-wave slowness perturbation in respect to the initial velocity model over the whole depth range.

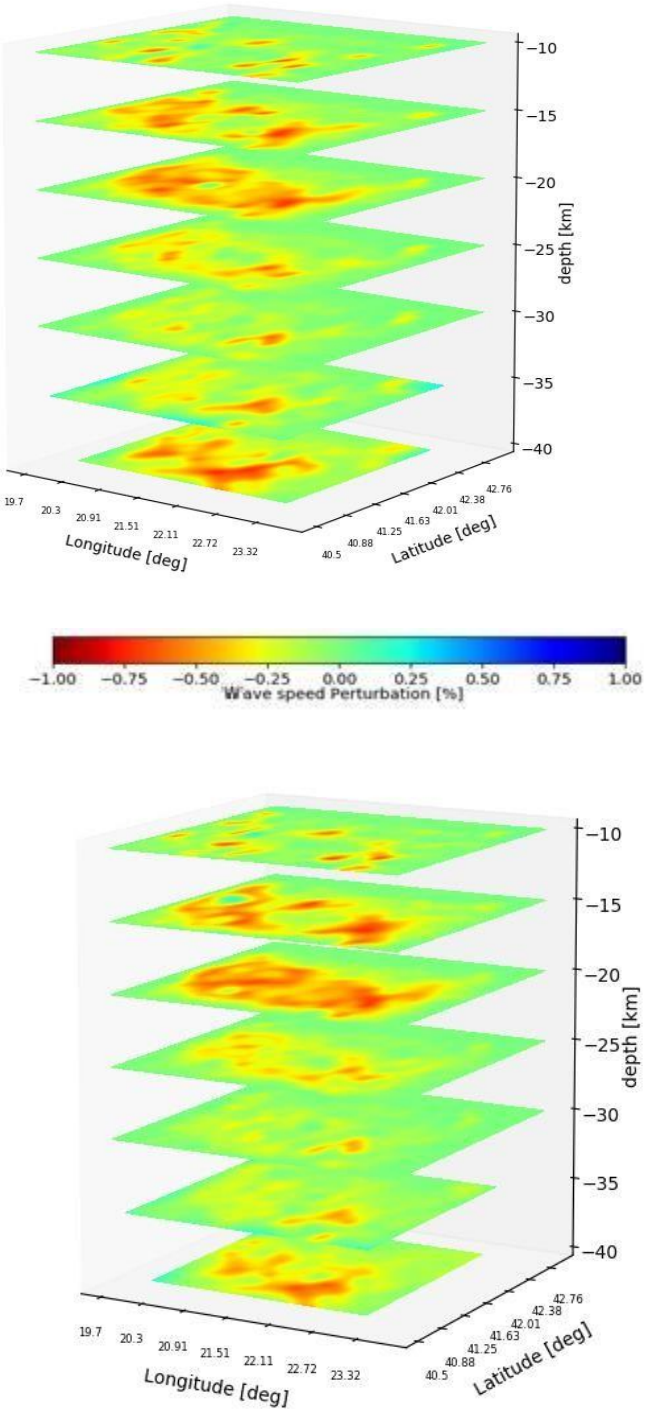

Figure 10: Horizontal P-wave (top) and S-wave (bottom) slowness perturbation images at depth.

Patterns on the horizontal images for both P-wave and S-wave cases point to an overall East-West directivity, possibly due to the regional compression that has been widely discussed by many authors, for example Burchfiel, *et al.* (2006). The most northerly parts and the most easterly parts

of the cuboid have very little data to change the background velocity, consequently the resulting model there contains artefacts.

Macedonia is a complex geological, tectonic and seismotectonic environment with zones of high seismicity. In order to interpret the results with the geology, these tomographic images of the first layer were superimposed on the topography map. Figure 11 shows a combined image of the Pwave relative perturbation image for 0-5 km and the topography. It can be seen that the zones with slower velocity correlate well with the edges between the valleys and the mountains ranges. That is especially consistent with the seismic zones Skopje, Ohrid and Pehcevo, depicted with circles, where the strongest and most damaging earthquakes occurred in the last hundred years.

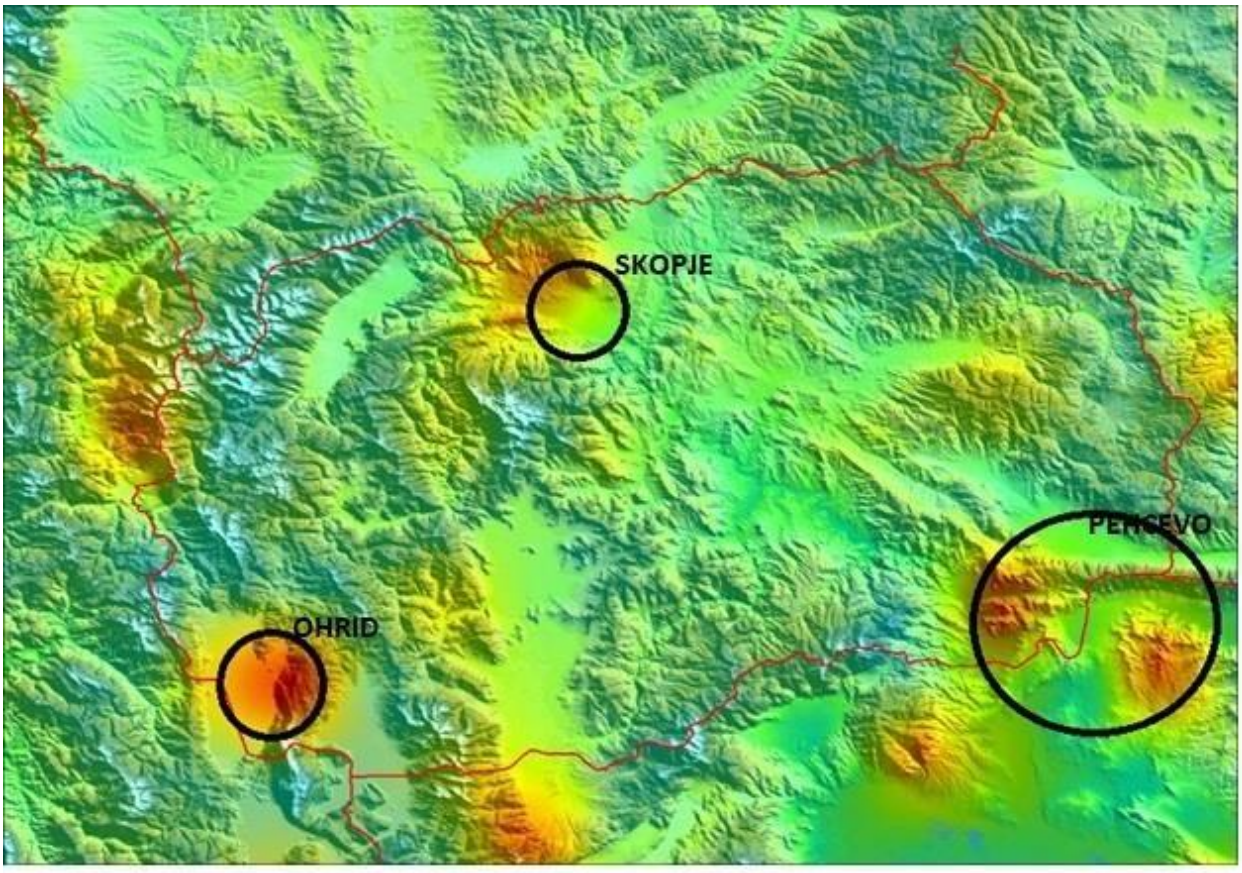

Figure 11: Combined horizontal P-wave slowness perturbation image at 0-5 km and topography of Macedonia. The circles represent the zones of strong earthquakes over the last 100 years.

The tomography results in the vertical slices through the cuboid along the selected latitudes and longitudes reveal more details of the lithosphere under specific regions. In the 1980's large scale experiments were made across Macedonia and profiles were produced with the seismic method known as Deep Seismic Sounding (DSS). For instance, Fig. 12 shows the latitudinal slice near 41^{o}N and superimposed seismic profile after Pekevski *et al.,* (2009), adapted from the original velocity model by Arsovski and Petkovski (1975) The images extended in depth underneath the Ohrid area (20.75^{o}E) on the western side and the Pehchevo (23^{o}E) to the east, match the previously

proposed model and faulting maps for the central part of the Balkan Peninsula obtained by applying geostatistical procedures (Boykova, 1995).

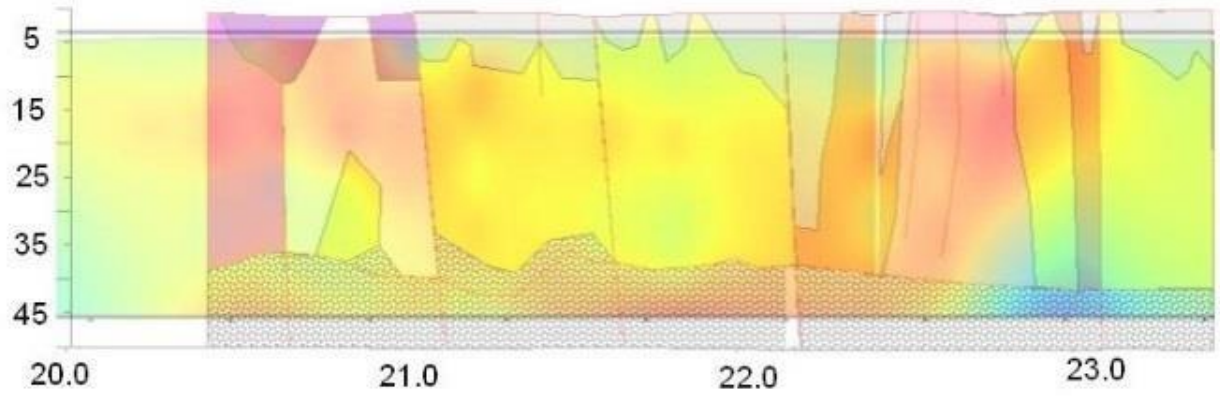

Figure 12: Combined seismic profile and the slowness perturbation image for a vertical latitudinal slice near 41^{o}N.

Longitudinal and latitudinal vertical slices through the cuboid at various angles can assist in detecting the more localized stress regime in Macedonia, as well as an estimate of the depth of the Moho discontinuity. From those combined images, the Moho depth of around 35 km under the Ohrid seismic station is in very close agreement with the values produced by receiver function methods (Petkovski *et al.,* 2009). Since the parts of the cuboid edges and depths greater than 45 km are not properly covered by the seismic rays, those sections may experience artefacts of the tomography process.

5 DISCUSSION AND SUMMARY

The tomographic studies of PNG and Macedonia is a work in-progress. The authors hope to continue in more details as soon as new data become available when the 3-D variations to the velocity models will be further explored. The main aim here was to demonstrate the possibilities of geotomography as a tool to investigation of the crustal shape and structure in specific tectonic regions.

Although at the edge of the Australian Moho map constructed from the full set of available seismological estimates, our geotomography images are in agreement with other authors for areas underneath the Southern Highlands of PNG (for example Drummond *et al.*, 1979). The horizontal images are consistent with compression in a north-south direction, with a gently folded belt in between. From the vertical slices, the estimated Moho depth is approximately 40 km, though influenced by the limited source-receiver geometry. The results in the combined slices of the cuboid within the station network show on the southern side a low velocity zone coinciding with the known volcano Mt. Bosavi, with its imprint extending down to 20 km, after which depth the image become less clear.

For the territory of Macedonia, which is part of the Southern Balkan Extensional Regime (Burchfiel *et al.*, 2006), tomographic images confirm the complex geological and seismotectonic environment. The inversion results can be interpreted from several perspectives, and depending on the discretization cell size of the model may reveal geological features of potential interest.

Patterns on the horizontal images for both P-wave and S-wave inversion point to an overall East-West directivity, with zones of slower velocity that correlate well with the edges between the valleys and the mountains ranges. That is evident with the seismic zones for Skopje, Ohrid and Pehcevo, where the strongest and most damaging earthquakes happened historically.

The vertical longitudinal and latitudinal slices through the cuboid and at various angles can assist in detection of the more localized stress regime in Macedonia, as well as the estimate of the depth of the Moho discontinuity.

3-D models and cross-sections of the crust produced by this new methodology show the potential of the geotomography application in revealing velocity perturbation on both local and regional scale. The new images should contribute towards better understanding of the seismicity and tectonics in the regions and improvement of earthquake hazard assessments.

6 ACKNOWLEDGEMENT

The authors want to acknowledge the Australian Earthquake Engineering Society for allowing the usage of data collected from the PNG experiment and Oil Search for providing logistic support in Papua New Guinea, and the staff of the Seismological Observatory in Skopje, for assembling the event catalogues for the Macedonian region.

7 REFERENCES

Arsovski, M., and Petkovski, R., (1975). Neotectonics of SR Macedonia, Publication 49, IZIIS, Skopje, R. Macedonia.

Boykova, A.: (1995). Moho discontinuity in central Balkan Peninsula in the light of the geostatical structural analysis, Physics of the earth and planetary interiors, v. 114, pp. 49-58.

Burchfiel, B.C., King, R.W., Todosov., A., Kotzev, V., Durmurdzanov, N., Serafimovski, T., and Nurce, B., (2006). GPS results for Macedonia and its importance for the tectonics of the Southern Balkan extensional regime, Tectonophysics, 413, pp. 239-248.

Drummond, B.J., Collins, C.D.N. and G. Gibson, G. (1979). The crustal structure of the Gulf of Papua and northwest Coral Sea. BMR Journal of Australian Geology & Geophysics, v4, pp: 341·351.

Gibson, G., McCue, K.F. and Love, D. (2018). Aftershocks, Crustal Structure and Faulting along the Southern Side of the Central Highlands, Papua New Guinea. Australian Earthquake Engineering Society AEES Conference, Perth, WA, Australia.

Kennett, B.L.N. and Abdullah, A. (2011). Seismic wave attenuation beneath the Australasian region. Australian Journal of Earth Sciences, Vol. 58, pp 285–295.

Pekevski, L., Dojcinovski, D., Panza, G.F., Vacari, F., and Romaneli, F. (2009). Neodeterministic Seismic Hazard Analysis of the Territory of Republic of Macedonia. International Centre for Theoretical Physics November Seminar, Trieste, Italy.

Petkovski, S., Tkalcic, H., and Pekevski, L. (2009). Structure of the Lithosphere beneath Macedonia from Teleseismic Receiver Functions. American Geophysical Union meeting, San Francisco, CA., US.

Sinadinovski, C., McCue, K.F., Gibson, G., Abdullah, A. and Love, D. (2019). AEES Reconnaissance Mission to Papua New Guinea, Pacific Conference on Earthquake Engineering, April 4-6, 2019, Auckland, New Zealand.